PHYSICAL REVIEW E, VOLUME 64, 025202(R)

Chaotic self-trapping of a weakly irreversible double Bose condensate

P. Coullet* and N. Vandenberghe
Institut Non-Lineaire de Nice, 1361 Route des Lucioles, 06560, Valbonne, France
(Received 16 January 2001; published 19 July 2001)

We analyze the dynamics of a weakly open Bose-Einstein condensate trapped in a double-well potential. Close to the self-trapping bifurcation, numerical simulations of the weakly irreversible one-dimensional Gross Pitaevskii equation reveal chaotic behaviors. A two-mode model is used to derive amplitude equations describing the complex dynamic of the condensate.

DOI: 10.1103/PhysRevE.64.025202 PACS number(s): 05.45.Ac, 89.75.Kd, 47.20.Ky, 03.75.Fi

Seventy years after its prediction, Bose-Einstein condensation has been observed in trapped gases of rubidium [1], sodium [2], and lithium [3]. The mean-field theory (Gross-Pitaevskii equation) has been quite successful in reproducing quantitatively many experimental observations [4].

We consider a weakly open thin cigar shaped Bose-Einstein condensate in a double-well potential described by the weakly dissipative version of the Gross-Pitaevskii (GP) equation,

$$i\partial_t\psi(x,t)=(V_{ext}(x)-\nabla^2+c_{nl}|\psi(x,t)|^2)\psi(x,t) + i\epsilon(\tilde{\alpha}-\tilde{\beta}_2|\psi(x,t)|^2+\tilde{\gamma}\nabla^2)\psi(x,t), \quad (1)$$

where $\psi(x,t)$ is the condensate wave function, and $V_{ext}(x)=ax^2+b(\exp(-cx^2)-1)$, is the trapping potential. The coefficient c_{nl} measures the interaction between the atoms of the condensate. The magnitude of the irreversible effects, which will be described later, is represented by ϵ.

A numerical simulation of Eq. (1) using finite differences discretization in space and a Crank-Nicholson scheme in time, shows that the condensate exhibits Lorenz-like chaotic behavior [5] (see Fig. 1). This paper aims to explain such a behavior.

In the case of a condensate with attractive atoms, the self-trapping instability is the result of the competition between the focusing of the wave function of the ground state at the center of the trap and the repulsive effect of the energy barrier. In the case of a condensate with repulsive atoms, a similar competition occurs for the first excited state, the black soliton [6,7], which, in the absence of barrier, is also localized at the center of the trap. The self-trapping bifurcation is a reversible pitchfork bifurcation that leads to two stable nonsymmetric states.

This bifurcation was first predicted in the frame of a drastic truncation of the GP equation, the two-mode model [8–10]. In order to check the prediction of this model, a detailed numerical analysis of the stationary solutions $\Psi(x,t)=f(x)\exp(-i\omega t)$ of the reversible Gross-Pitaevskii equation [$\epsilon=0$ in Eq. (1)] has been performed. The stability of the stationary solutions (Fig. 2) confirms the existence of a pitchfork bifurcation.

Although there is no rigourous reduction of the GP model to the two-mode model [8,9], such a model has been very useful in particular to predict the self-trapping bifurcation. In this letter we will use it as a toy model to investigate analytically the fate of the self-trapping instability in weakly open condensate. The two-mode model reads

$$i\partial_t\Psi_1=U|\Psi_1|^2\Psi_1-K\Psi_2, \quad (2a)$$

$$i\partial_t\Psi_2=U|\Psi_2|^2\Psi_2-K\Psi_1, \quad (2b)$$

where $\Psi_{1,2}$ represent the ground-state amplitudes in the two wells, U measures the atomic interaction ($U<0$ in the attractive case and $U>0$ in the repulsive case), and K the tunneling coupling parameter.

These equations admit two simple solutions of interest. The in-phase solution

$$\Psi_1^+=\Psi_2^+=\sqrt{\rho}\exp(i(-U\rho+K)t)$$

corresponds to the ground state. The antiphase solution

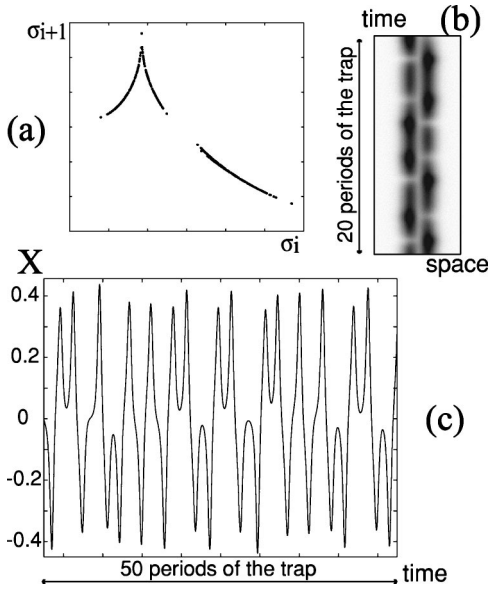

FIG. 1. Numerical solutions of Eq. (1): $c_{nl}=-1$, $a=1$, $b=6$, $c=10$, $\alpha=6$, $\beta=8$, $\gamma=3$, and $\epsilon=0.01$. (a) Plot of the successive minima of the "mass" $\int|\Psi|^2dx$. (b) Density plot of $|\Psi|^2$ showing the characteristic time and length scale of the chaotic oscillations. (c) Plot of the center of inertia $X=\int x|\Psi|^2dx$ as a function of time.

*Also at l'Institut Universitaire de France, 103 boulevard Saint-Michel, 75005 Paris, France.

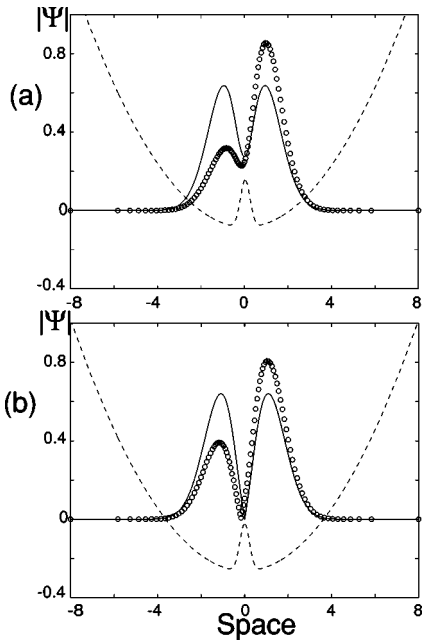

FIG. 2. Stationary numerical solutions of Eq. (1) with $\epsilon=0$. (a) $c_{nl}=-1$, the ground state and its nonsymmetric bifurcated state. (b) $c_{nl}=1$, the black soliton and its nonsymmetric bifurcated state. The dashed line represents the potential ($a=1$, $b=12$, $c=10$). The solid curve represents the symmetric unstable solution, the curve marked with ''o'' represents one of the two stable nonsymmetric solution.

$$\Psi_1^- = -\Psi_2^- = \sqrt{\rho}\exp(i(-U\rho-K)t)$$

corresponds to the dark soliton state. x_i and ϕ_i, $i=1,2$ are the amplitudes and phase perturbations of the in-phase and antiphase solutions

$$\Psi_1=(1+x_1)\exp(i\phi_1)\sqrt{\rho}\exp(i(-U\rho+\xi K)t), \quad (3a)$$

$$\Psi_2=\xi(1+x_2)\exp(i\phi_2)\sqrt{\rho}\exp(i(-U\rho+\xi K)t), \quad (3b)$$

where $\xi=1$ (resp. $\xi=-1$) for the in-phase solution (respectively antiphase solution). The use of the new variables $\sigma=x_1+x_2$, $\delta=x_2-x_1$, and $\phi=\phi_2-\phi_1$ simplifies Eqs. (2) to

$$\partial_t\sigma=-\xi K\delta\sin\phi, \quad (4a)$$

$$\partial_t\delta=2\xi K\sin\phi+\xi K\sigma\sin\phi, \quad (4b)$$

$$\partial_t\phi=-U\rho\delta(2+\sigma)+\xi K\left(\frac{2+\sigma-\delta}{2+\sigma+\delta}-\frac{2+\sigma+\delta}{2+\sigma-\delta}\right)\cos\phi. \quad (4c)$$

The invariance of these equations under the transformation $\xi\to-\xi$, $U\to-U$, $\delta\to\delta$, allows us to restrict our analysis to the attractive case ($U=-1$) without loss of generality. The linearization of Eqs. (4) reads

$$\partial_t\sigma=0, \quad (5a)$$

$$\partial_t\delta=2\xi K\phi, \quad (5b)$$

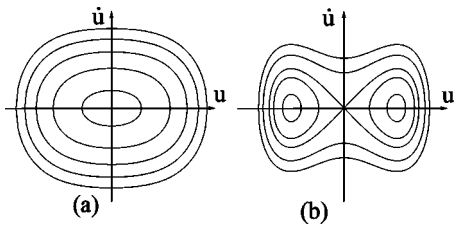

FIG. 3. Phase space (u,v) of Eqs. (6) with $w_0=0$. (a) $\lambda=-0.2$, (b) $\lambda=0.5$.

$$\partial_t\phi=2(\rho-\xi K)\delta. \quad (5c)$$

The antiphase solution ($\xi=-1$) is always stable in that case and the in-phase solution ($\xi=1$) loses its stability when $K<K_c=\rho$. Close to the instability, the variables scale with the small parameter $\lambda=4K_c(K-K_c)$, which measures the distance from the instability threshold. The scalings are the following: $\partial_t\sim O(\lambda^{1/2})$, $\sigma\sim O(\lambda)$, $\delta\sim O(\lambda^{1/2})$, and $\phi\sim O(\lambda)$. In the limit where $\lambda\to0$, Eqs. (4) asymptotically reduce to

$$\ddot{u}-(\lambda+w)u+u^3=0, \quad (6a)$$

$$\dot{w}=0, \quad (6b)$$

where $\delta=1/\sqrt{2}K_c u$, $\phi=1/2\sqrt{2}K_c^2 v$, and $\sigma=1/4K_c^2 w-1/8K_c^2u^2$.

These equations catch the universal features of the self-trapping transition (See Fig. 3). The instability can be achieved either by decreasing the coupling parameter K or by increasing the total number of atoms in the trap. This instability was depicted in [10], where the authors used elliptic functions to describe symmetric and nonsymmetric oscillations in the two-mode model. Equations (6) can be deduced directly from the GP model [11].

Inelastic collisions cause the decay of the condensate [12–15]. Once the condensate is formed, there is a flux of particles from the nonequilibrium above-condensate cloud to the condensate that tends to maintain a fixed number of condensed atoms: this is the pumping process. These effects can be included in the GP equation giving Eq. (1) [16]. The term $\tilde{\gamma}\nabla^2\Psi$ represents diffusion. The corresponding modified two-mode model becomes

$$i\partial_t\Psi_1=U|\Psi_1|^2\Psi_1-K\Psi_2+i\epsilon I_1, \quad (7a)$$

$$i\partial_t\Psi_2=U|\Psi_2|^2\Psi_2-K\Psi_1+i\epsilon I_2, \quad (7b)$$

where

$$I_{1,2}=\alpha\Psi_{1,2}-\beta_2|\Psi_{1,2}|^2\Psi_{1,2}+\gamma\Psi_{2,1}, \quad (8)$$

where α represents the feeding rate of the condensate and $\beta_2|\Psi_{1,2}|^2$, its decay rate induced by the inelastic two body collisions, and γ describes the irreversible small coupling between the condensates due to inhomogeneous effects and diffusion. The irreversible terms in the two-mode model can be computed from Eq. (1), using an ansatz based on two ground states of the isolated traps [9]. Though these effects

are small, they will dramatically affect the dynamic close to the self-trapping instability. Eqs. (5) become

$$\partial_t \sigma = -K\delta \sin\phi + \epsilon D_\sigma, \tag{9a}$$

$$\partial_t \delta = 2K \sin\phi + K\sigma \sin\phi + \epsilon D_\delta, \tag{9b}$$

$$\partial_t \phi = -\rho\delta(2+\sigma) + K\left(\frac{2+\sigma-\delta}{2+\sigma+\delta} - \frac{2+\sigma+\delta}{2+\sigma-\delta}\right)\cos\phi + \epsilon D_\phi, \tag{9c}$$

where the dissipative terms are

$$D_\sigma = (1+x_1)[\alpha - \beta_2\rho(1+x_1)^2] + (1+x_2) \times [\alpha - \beta_2\rho(1+x_2)^2] + \gamma(2+x_1+x_2)\cos\phi, \tag{10a}$$

$$D_\delta = (1+x_1)[\alpha - \beta_2\rho(1+x_1)^2] - (1+x_2) \times [\alpha - \beta_2\rho(1+x_2)^2] + \gamma(x_2-x_1)\cos\phi, \tag{10b}$$

$$D_\phi = -\gamma\left(\frac{1+x_1}{1+x_2} + \frac{1+x_2}{1+x_1}\right)\sin\phi, \tag{10c}$$

and $x_1 = \frac{1}{2}(\sigma-\delta)$ and $x_2 = \frac{1}{2}(\sigma+\delta)$.

We can adjust the order of magnitude of the bifurcation parameter λ to the amplitude of the small irreversible effects. Close to the self-trapping instability, using the same asymptotic as in the reversible case, with $\epsilon \sim O(\lambda^{\frac{1}{2}})$, we then derive a new set of equations:

$$\ddot{u} - (\lambda' + w)u + \nu\dot{u} + u^3 = 0, \tag{11a}$$

$$\dot{w} = -\mu w - \eta u^2, \tag{11b}$$

where $\lambda' = 4K_c(K_c - K) + 2\epsilon^2\gamma(\alpha - \gamma - 3\beta_2\rho)$, $\delta = 1/\sqrt{2}K_c u$, $\phi = 1/2\sqrt{2}K_c^2 v + \epsilon\alpha 1/\sqrt{2}K_c^2 u$, $\sigma = 1/4K_c^2 w - 1/8K_c^2 u^2$, and $K_c = \alpha + \gamma/\beta_2$. Irreversible effects are captured by the parameters μ, ν, and η. The parameter $\nu = \epsilon(2\alpha + 6\gamma)$ measures the damping of the oscillations of the center of inertia of the condensate, $\mu = 2\epsilon(\alpha+\gamma)$ measures the loss of atoms due to the inelastic two body collisions, and $\eta = \epsilon(4\alpha + 6\gamma)$ measures the ''stimulated'' loss of atoms induced by the symmetry breaking. This last term gives rise to the complex behavior, since it couples the equations of the dynamic. These equations can be deduced directly from the irreversible GP model [Eq. (1)] without the intermediate step of the two-mode model. The coefficients (λ', μ, ν, and η) are then numerical quantities that are computed from the eigenfunctions of the linearized GP equations [11].

As shown in [17], Eqs. (11) are equivalent to the Lorenz equations. They possesses complicated dynamical solutions that are likely to be observed in condensates. A typical solution of the weakly irreversible two-mode model is shown on Fig. 4(a).

The chaotic alternation between self-trapped states of opposite sign is a typical behavior of the Lorenz model. The plot of the successive maxima of the total number of condensed atoms reveals the chaotic structure of the Lorenz attractor [Fig. 4(b) and Fig. 1].

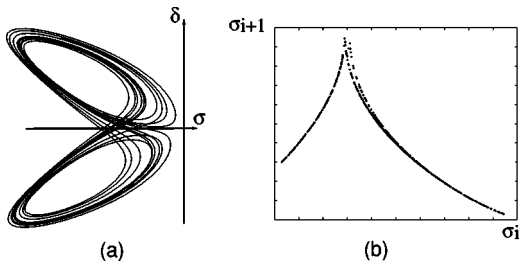

FIG. 4. (a) Projection in the plane $(\sigma-\delta)$ of a typical chaotic solution of Eqs. (9) for parameters $U=-1$, $K=1.175$, $\epsilon=0.05$, $\alpha=1$, $\beta_2=1$, $\beta_3=0$, $\gamma=0.2$; (b) Plot of the successive maxima of σ.

The origin of the chaotic behaviors can be understood qualitatively. The dissipation and the forcing affect dramatically the dynamics near the self-trapping instability. First the stationary self-trapped state is selected among all the solutions of the conservative dynamical system. Second, when the number of atoms becomes larger than a critical value, the self-trapped state can lose its stability because the density becomes so high in a given well that the dissipation leads to the drop in the number of atoms in the condensate. This effect tends to stabilize the symmetrical state where the number of condensed atoms grows again. But because of the inertia, the center of mass of the condensate can move to the other well. This dynamical process can continue forever, giving rise to oscillations of the center of inertia of the condensate in a potential well separated by an abrupt change to the other well.

Despite their weaker thermodynamical stability, trapped gases with attractive interactions appear to be one of the candidate for such an investigation, since in this case the ground state itself experiences the self-trapping instability. The number of atoms in the trap is supposed to be small enough for the quantum tunneling and the temperature effects to be neglected [18]. Once the condensate is formed, a laser sheet with a very low intensity is applied in order to separate the condensate into two parts. As the intensity of the laser increases (the tunneling parameter of the two-mode model K decreases), the self trapping instability leads to a steady state characterized by different populations of atoms between the two condensates $(\sigma \neq 0)$. As the intensity decreases further, a time-dependent regime that eventually leads to regular or chaotic alternation between the two self trapped states will appear. In the case of a trapped gas with repulsive interactions, the similar scenario should be observed when the initial state is a black soliton [6,7]. The variation of the nonlinearity as proposed in [19] is another accurate experimental protocol that can be used in order to observe the chaotic behaviors described in this letter.

The value of the dissipative coefficients appearing in Eq. (1) are really difficult to estimate. The values of dissipation strongly depend on the temperature [20] of the condensate, but are smaller than one. For the simulation of Fig. 1, we took $\epsilon\alpha/\sqrt{a}$ (where $\sqrt{a}$ is the frequency of the trap) equal to

0.06, which gives a time scale for losses close to the time scale observed in classical experiments [21]. The intensity and the width of the laser sheet is easily tunable in experiment and it would be easy to adjust it in order to approach the self-trapping bifurcation. For the realistic value of Fig. 1, the characteristic length and time scales can be seen on Fig. 1(b).

We have demonstrated that an open Bose condensate can experience a transition to chaos. Although most of our analysis is based on the approximate two-mode model, our conclusions are independent of this model. The nature of the irreversible effects (two-body or three-body recombination) is not crucial in our analysis, since they only contribute to actual values of the macroscopic friction parameters of the Lorenz equations.

Numerical simulations have been performed thanks to the NLKit software developed at the INLN.

[1] M. H. Anderson, J. R. Ensher, M. R. Matthews, C. E. Wieman, and E. A. Cornell, Science **269**, 198 (1995).
[2] K. B. Davis, M. O. Mewes, M. R. Andrews, N. J. van Druten, D. S. Durfee, D. M. Kurn, and W. Ketterle, Phys. Rev. Lett. **75**, 3969 (1995).
[3] C. C. Bradley, C. A. Sackett, J. J. Tollett, and R. G. Hulet, Phys. Rev. Lett. **75**, 1687 (1995).
[4] F. Dalfovo, S. Giorgini, L. P. Pitaevkii, and S. Stringari, Rev. Mod. Phys. **71**, 463 (1999) and references therein.
[5] E. N. Lorenz, J. Atmos. Sci. **20**, 130 (1963).
[6] J. Denschlag, J. E. Simsarian, D. L. Feder, C. W. Clark, L. A. Collins, J. Cubizolles, L. Deng, E. W. Hagley, K. Helmerson, W. P. Reinhardt, S. L. Rolston, B. I. Schneider, and W. D. Phillips, Science **287**, 197 (2000).
[7] S. Burger, K. Bongs, S. Dettmer, W. Ertmer, K. Sengstock, A. Sanpera, G. V. Shlyapnikov, and M. Lewenstein, Phys. Rev. Lett. **83**, 5198 (1999).
[8] G. J. Milburn, J. Corney, E. M. Wright, and D. F. Walls, Phys. Rev. A **55**, 4318 (1997).
[9] S. Raghavan, A. Smerzi, S. Fantoni, and S. R. Shenoy, Phys. Rev. A **59**, 620 (1999).
[10] A. Smerzi, S. Fantoni, S. Giovanazzi, and S. R. Shenoy, Phys. Rev. Lett. **79**, 4950 (1997).
[11] P. Coullet and N. Vandenberghe, e-print INLN.
[12] M. Edwards, R. J. Dodd, C. W. Clark, P. A. Ruprecht, and K. Burnett, Phys. Rev. A **53**, R1950 (1996).
[13] P. O. Fedichev, M. W. Reynolds, and G. V. Shlyapnikov, Phys. Rev. Lett. **77**, 2921 (1996).
[14] T. W. Hijmans, Y. Kagan, G. V. Shlyapnikov and J. T. M. Walraven, Phys. Rev. B **48**, 12 886 (1993).
[15] A. J. Moerdijk, H. M. J. M. Boesten, and B. J. Verhaar, Phys. Rev. A **53**, 916 (1996).
[16] Y. Kagan, A. E. Muryshev, and G. Shlyapnikov, Phys. Rev. Lett. **81**, 933 (1998).
[17] M. Clerc, P. Coullet, and E. Tirapegui, Phys. Rev. Lett. **83**, 3820 (1999).
[18] C. A. Sackett, H. T. C. Stoof, and R. G. Hulet, Phys. Rev. Lett. **80**, 2031 (1998).
[19] S. L. Cornish, N. R. Claussen, J. L. Roberts, E. A. Cornell, and C. E. Wieman, Phys. Rev. Lett. **85**, 1795 (2000).
[20] D. M. Stamper-Kurn, H.-J. Miesner, S. Inouye, M. R. Andrews, and W. Ketterle, Phys. Rev. Lett. **81**, 500 (1998).
[21] B. Kneer, T. Wong, K. Vogel, W. P. Schleich, and D. F. Walls, Phys. Rev. A **58**, 4841 (1998).